Fission Fragment Angular Momenta: Generation and Observation

Jørgen Randrup[1,*], *Thomas* Døssing[2], and *Ramona* Vogt[3,4]

[1]Nuclear Science Division, Lawrence Berkeley National Laboratory, Berkeley, California, USA
[2]Niels Bohr Institute, University of Copenhagen, Copenhagen, Denmark
[3]Physics Division, Lawrence Livermore National Laboratory, Livermore, California, USA
[4]Department of Physics, University of California, Davis, USA

Abstract. The fission fragment angular momenta can generally be expressed in terms of the six normal modes of rotation for the dinucleus and different models populate those modes to different degrees reflecting the mechanisms involved. For the nucleon exchange mechanism, the characteristic time scales for the various modes are discussed, leading to the expectation that the wriggling mode is fully populated, while twisting is unlikely to play a major role; bending probably has some presence which increases with mass asymmetry. Subsequently it is discussed how information about the fragment spin directions can be determined by observation of $E2$ emissions in even-even nuclei. It is shown how the yield ratio $Y(0^\circ)/Y(90^\circ)$ in a modern Wilhelmy-type experiment can reveal the degree of twisting, a measurement that could be readily carried out now. Furthermore, with a view towards the future when the required technology has been developed, it is illustrated how the relative role of positive modes (wriggling) and negative modes (bending and twisting) can be determined by measuring the opening angle between two $E2$ photons whose helicities are also identified.

1 Introduction

The generation of the fission fragment angular momenta and their observational effects are currently under intense study. It was shown long ago, from the distribution of identified $E2$ photons relative to the fragment motion, that the angular momenta of the primary fragments tend to be perpendicular to the fission axis [1]. Quite recently it was shown that the observed mass dependence of the spin magnitudes [2] are consistent with a statistical population of the rotational modes at scission [3].

Here we show that the nucleon exchange mechanism populates the dinuclear wriggling mode quite quickly, whereas the twisting mode is populated rather slowly, with the bending mode being somewhat intermediate. Subsequently, we discuss how suitable photon measurements may provide information about the directions of the fragment angular momenta, either with respect to the fission axis or relative to one another, and how such measurements may help to determine the relative presence of the various rotational modes at the time of scission. A more detailed discussion was given in Ref. [4].

2 Modes of rotation in the dinucleus

Due to angular-momentum conservation, the angular momenta of the fission fragments, $\boldsymbol{S}_L$ and $\boldsymbol{S}_H$, are coupled to that of the relative fragment motion, $\boldsymbol{L}$, so that the total angular momentum, $\boldsymbol{S}_0 = \boldsymbol{S}_L + \boldsymbol{S}_H + \boldsymbol{L}$, is conserved. Thus a binary system has six intrinsic modes of rotation in terms of which its rotational energy can be expressed [4],

$$E_0^{\rm rot} = \frac{S_0^2}{2\mathcal{I}_0} + \frac{s_{\rm wrig}^2}{2\mathcal{I}_{\rm wrig}} + \frac{s_{\rm bend}^2}{2\mathcal{I}_{\rm bend}} + \frac{s_{\rm twst}^2}{2\mathcal{I}_{\rm twst}} + \frac{s_{\rm tilt}^2}{2\mathcal{I}_{\rm tilt}}\,. \quad (1)$$

The various normal modes were imaginatively named by Nix and Swiatecki [5] as *wriggling* and *bending* (in which the two fragment spins are perpendicular to the symmetry axis $\hat{\boldsymbol{R}}$) and *twisting* and *tilting* (in which the spins are parallel to $\hat{\boldsymbol{R}}$). The various moments of inertia are

$$\mathcal{I}_0 = \mathcal{I}_{LH} + \mathcal{I}_R, \;\; \mathcal{I}_{\rm wrig} = \mathcal{I}_{LH}\mathcal{I}_R/\mathcal{I}_0, \quad (2)$$

$$\mathcal{I}_{\rm bend} = \mathcal{I}_{\rm twst} = \mathcal{I}_L\mathcal{I}_H/\mathcal{I}_{LH}, \;\; \mathcal{I}_{\rm tilt} = \mathcal{I}_{LH}. \quad (3)$$

where $\mathcal{I}_R = \mu R^2$ is the moment of inertia for the relative motion and $\mathcal{I}_{LH} \equiv \mathcal{I}_L + \mathcal{I}_H$.

The two fragment spins $\boldsymbol{S}_{\rm f}$ receive contributions from each of the six normal modes $\boldsymbol{s}_m$, so $\boldsymbol{S}_{\rm f} = (\mathcal{I}_{\rm f}/\mathcal{I}_0)\boldsymbol{S}_0 + \delta\boldsymbol{S}_{\rm f}^{\rm wrig} + \delta\boldsymbol{S}_{\rm f}^{\rm bend} + \delta\boldsymbol{S}_{\rm f}^{\rm twst} + \delta\boldsymbol{S}_{\rm f}^{\rm tilt}$. With $+/-$ for the light/heavy fragment, the individual fragment spin contributions are given in terms of the normal modes $\boldsymbol{s}_m$ by

$$\delta\boldsymbol{S}_{\rm f}^{\rm wrig} = (\mathcal{I}_{\rm f}/\mathcal{I}_{LH})\,\boldsymbol{s}_{\rm wrig}, \;\; \delta\boldsymbol{S}_{\rm f}^{\rm bend} = \pm\boldsymbol{s}_{\rm bend}, \quad (4)$$

$$\delta\boldsymbol{S}_{\rm f}^{\rm twst} = \pm\boldsymbol{s}_{\rm twst}, \;\; \delta\boldsymbol{S}_{\rm f}^{\rm tilt} = (\mathcal{I}_{\rm f}/\mathcal{I}_{\rm tilt})\,\boldsymbol{s}_{\rm bend}. \quad (5)$$

A statistical ensemble can be generated by sampling the amplitudes s_m from thermal distributions, $P(s_m) \sim \exp(-s_m^2/2\mathcal{I}_m T)$, and then construct the fragment spins $\boldsymbol{S}_{\rm f}$.

The contributions to the fragment spins from each of the two degenerate wriggling modes, as well as from the tilting mode, are parallel, while those from each of the two degenerate bending modes, as well as from the twisting mode, are opposite, as illustrated in Fig. 1:

*e-mail: JRandrup@LBL.gov

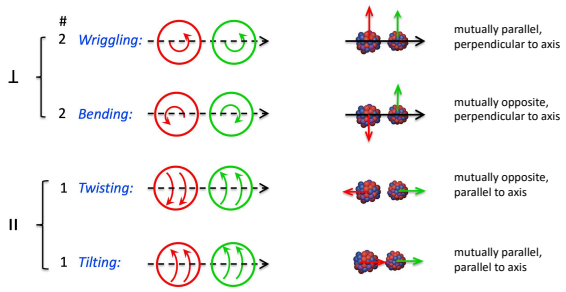

Figure 1. Illustration of the six normal modes of rotation in a disphere. The *wriggling* and *bending* modes involve rotations perpendicular to the symmetry axis connecting the two centers (and these modes are therfore doubly degenerate), while the *twisting* and *tilting* modes involve rotations parallel to the symmetry axis. In wriggling and tilting the two angular momenta are parallel, while they are opposite in bending and twisting.

3 Angular momentum dynamics

As the fissioning system evolves beyond the saddle shape, it gradually attains an ever more binary character and the dinuclear modes may then become agitated. Because the rates of agitation of the different rotational modes depend on the physical mechanisms involved, the degree to which the modes are populated can reveal the nature of those mechanisms. It is therefore of interest to consider the associated relaxation times which for the mode m is given by $t_m = \mathcal{I}_m/M_m$, where $\mathcal{I}_m$ is the moment of inertia for the mode (see above) and M_m is its mobility coefficient. Generally, the time scale for exciting the tilting mode is very long [6] and this mode is therefore ignored here.

The generation of fragment angular momentum has been particularly well studied for the *nucleon exchange* mechanism [6, 7], quasi-elastic transfer of multiple individual nucleons. This mechanism yields the following expressions for the mobility coefficients $\{M_m\}$ [4, 6],

$$M_{\rm wrig} = m\mathcal{N}R^2, \tag{6}$$

$$M_{\rm bend} = m\mathcal{N}\left[\left(\frac{\mathcal{I}_H R_L - \mathcal{I}_L R_H}{\mathcal{I}_L + \mathcal{I}_H}\right)^2 + c_{\rm ave}^2\right], \tag{7}$$

$$M_{\rm twst} = m\mathcal{N}c_{\rm ave}^2\,. \tag{8}$$

Here the rate of nucleon transfers from one fragment to the other is given by $\mathcal{N} \approx \frac{1}{4}\rho\bar{v}\pi c^2$ [8] where ρ is the standard nucleon density, $\bar{v} = \frac{3}{4}v_F$ is the mean nucleon speed, and c is the neck radius. Furthermore, $c_{\rm ave}^2 = \frac{1}{2}c^2$ is the average of the transverse displacement across the neck. $M_{\rm twst}$ is an order of magnitude smaller than $M_{\rm wrig}$ because $c^2 \ll R^2$, so $t_{\rm twst} \gg t_{\rm wrig}$. The first term in $M_{\rm bend}$ vanishes for symmetric divisions, giving $M_{\rm bend} = M_{\rm twst}$, but $M_{\rm bend}$ is significantly larger than $M_{\rm twst}$ for typical mass divisions (and small neck radii). These relaxation times are shown in Fig. 2 as functions of c, using $R = R_L + R_H + d$ with $d = 4$ fm.

Figure 2 shows the resulting mode relaxation times t_m, plotted as functions of the neck radius c. These should be compared with $t_{\rm fiss}$, the time it takes the fissioning system to evolve from the first appearance of a dinuclear geometry to the rupture of the neck. We assume here that $t_{\rm fiss}$ is one to several times 10^{-21} s.

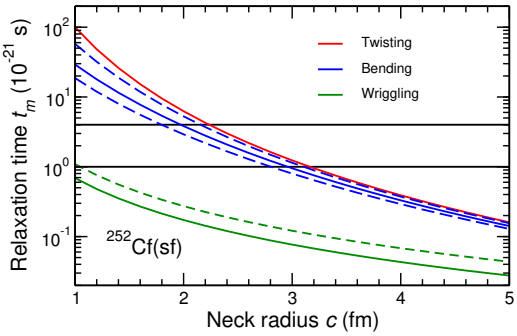

Figure 2. The calculated relaxation times t_m for wriggling, bending, and twisting, shown as functions of the neck radius c for a tip separation of $d = 4$ fm. For wriggling is also shown the result for touching spheres, $d = 0$ (dashed green). For bending, the solid curve is for the mass division 108:144 (the most probable), while the dashed curves are for 100:152 (lower) and 118:134 (upper) which are each half as probable. The two horizonthal lines show $t_{\rm fiss}$=1 zs and $t_{\rm fiss}$=4 zs. (From [4].)

The calculated $t_{\rm wrig}$ stays well below the assumed range of $t_{\rm fiss}$ and one should therefore expect that the wriggling mode maintains full equilibrium until the time of scission, which is expected to occur for $c \approx 2$ fm. By contrast, $t_{\rm twst}$ is likely similar to or longer than $t_{\rm fiss}$, so the twisting mode will adjust only slowly as scission is approached. However, in induced fission at higher energies it may gain more prominence. The bending mode is somewhat intermediate and is expected to be agitated to an appreciable degree, though likely not fully. However, because $t_{\rm bend}$ depends on the mass asymmetry, the degree of bending at scission should increase with the asymmetry.

These predicted features can be tested experimentally.

4 Photon measurements

We now explore the sensitivity of various photon observables to the degree of agitation of the various rotational modes. For this purpose, the angular momentum treatment described above has been incorporated into the fission simulation code FREYA [9–11]. At the time of scission, each of the normal modes m is sampled from a Boltzmann distribution with an effective mode temperature $T_m = c_m T_{\rm sc}$ where $T_{\rm sc}$ is the temperature of the dinuclear complex at scission; the coefficient c_m can be adjusted to allow exploration of different scenarios.

In order to illustrate the sensitivity of the observables to the degree of agitation of the various rotational modes, it is convenient to characterize a particular physical scenario by the mode suppression coefficients $(c_{\rm wrig}, c_{\rm bend}, c_{\rm twst})$. The standard version of FREYA uses $(c_{\rm wrig}, c_{\rm bend}, c_{\rm twst}) = (1, 1, 0)$, *i.e.* wriggling and bending are both fully agitated

while there is no twisting [9, 11]. (When other proportions are employed, the coefficients $\{c_m\}$ are renormalized to ensure that the magnitudes remain unchanged on average.)

The primary fragments separate along Coulomb trajectories, leading to two freely moving compound nuclei. The associated rotation of the dinuclear axis amounts to only a couple of degrees [9], so the free fragments are moving approximately along the direction of the fission axis. Subsequently, each fragment evaporates neutrons until its statistical excitation energy has fallen below the neutron separation energy, at which point the remaining excitation and rotation is disposed of by photon radiation.

We concentrate here on the sequential emission of collective $E2$ photons along the ground-state band in even-even product nuclei. The distribution of their polar angles $\theta_{\gamma S}$, relative to the fragment spin direction, is given by

$$P^2_{2,h}(\theta_{\gamma S}) = \tfrac{5}{2}\left(d^2_{2,h}(\theta_{\gamma S})\right)^2 = \tfrac{5}{8}(1+h\cos\theta_{\gamma S})^2\sin^2\theta_{\gamma S}, \quad (9)$$

where $d^2_{2,h}(\theta)$ is a Wigner d-function. We note that the photon helicity $h = \pm 1$ enters.

4.1 Angular distributions

It is experimentally possible to identify specific $E2$ transitions, a feature that can be used to identify the emitting product nucleus. To exploit this, we have selected a number of even-even product nuclei and henceforth focus on events that lead to those.

We consider here the angular distribution of the $E2$ photons relative to the direction of the emitting product nucleus. This observable is sensitive to the spin direction of the emitting nucleus. Thus, if the fragment spin was directed along the fragment motion, then the resulting angular distribution of the emitted $E2$ photons, in terms of $\mu \equiv \cos\theta_{\gamma f}$, where $\theta_{\gamma f}$ is the angle between the emission direction and the velocity of the emitter nucleus, would be sideways peaked [4],

$$W_{\parallel}(\theta_{\gamma f}) \sim 1 + hP_1(\mu) - \tfrac{5}{7}P_2(\mu) - hP_3(\mu) - \tfrac{2}{7}P_4(\mu). \quad (10)$$

However, a much more realistic scenario is that the spin of the emitting nucleus is perpendicular to the motion of the fragment. In that case the basic angular distribution, which is given in Eq. (9) in terms of the angle between the photon motion and the emitter spin, $\theta_{\gamma S}$, must be averaged over all the equally likely perpendicular directions of $\boldsymbol{S}$. The directional average removes the odd orders, and thereby also the helicity dependence, and the observable distribution in the perpendicular scenario becomes forwards-backwards peaked [4],

$$W_{\perp}(\theta_{\gamma f}) \sim 1 + \tfrac{5}{14}P_2(\mu) - \tfrac{3}{28}P_4(\mu), \quad (11)$$

which differs qualitatively from the distribution for the parallel scenario, Eq. (10).

Figure 3 shows the angular distribution $dN/d\cos\theta_{\gamma f}$ for two opposite assumptions about the population of the various dinuclear rotational modes, as obtained with the FREYA event-by-event simulation, namely purely perpendicular spins, (1,1,0), or purely parallel spins, (0,0,1). As a useful reference, the above idealized distributions $P_{\parallel}(\theta_{\gamma f})$ and $P_{\perp}(\theta_{\gamma f})$ are shown for each scenario. The results for the perpendicular scenario (1,1,0) are consistent with those obtained experimentally [1, 12]. However, those measurements were made over fifty years ago and have relatively large error bars. It is therfore not possible to exclude the presence of some twisting on that basis and it is of interest to repeat the experiment with modern detectors that yield more accurate results. It might then be possible to discern how much twisting is present at scission.

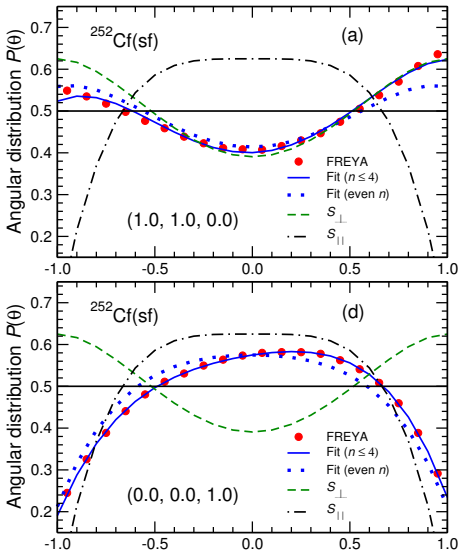

Figure 3. The angular distribution of the collective $E2$ photons relative to the direction of the emitting product nucleus for two opposite scenarios: The standard FREYA scenario, in which the perpendicular modes (wriggling and bending) are fully agitated, while the parallel mode (twisting) is absent (a) and the extreme scenario in which only twisting is present (d). The specified values of $(c_{\rm wrig}, c_{\rm bend}, c_{\rm twst})$ are indicated for each scenario. The Legendre fits (solid curves) and their symmetric parts (dots) are shown, as are the distributions for perfectly perpendicular or perfectly parallel emitter spins. (From Ref. [4].)

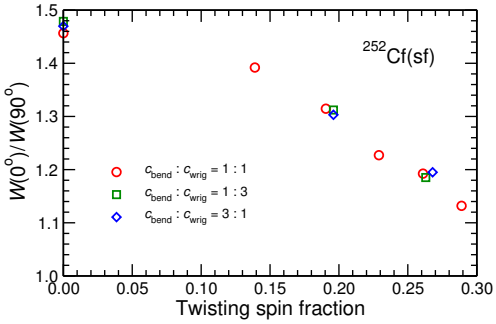

Figure 4. The ratio of the $E2$ photon yield in the direction of the fragment motion, $W(0°)$, and the transverse yield, $W(90°)$, shown as a function of the coefficient $c_{\rm twst}$ controlling the population of the twisting mode, $T_{\rm twst} = c_{\rm twst}T_{\rm sc}$. The result for three different relative proportions of wriggling and bending are shown at several degrees of twisting, illustrating the weak dependence on the mix of wriggling and bending. (From [4].)

A suitable observable for determining the degree of twisting may be the $W(0°) : W(90°)$ yield ratio, the forward yield relative to the sidewards yield. This is illustrated in Fig. 4 showing the yield ratio as a function of the relative presence of twisting, as measured by the suppression coefficient $c_{\rm twst}$. There is a pronounced decrease as $c_{\rm twst}$ is increased from zero to one and it is noteworthy that even a visually small change in $dN/d\cos\theta$, as when going from no twisting to 20% twisting, produces a significant decrease in the yield ratio. It is also important that the yield ratio, while quite sensitive to $c_{\rm twst}$, is practically independent of the relative proportion of wriggling and bending: The results for three very different values of $c_{\rm bend} : c_{\rm wrig}$ lead to very similar angular distributions and hence to nearly identical yield ratios which is thus exclusively sensitive to the degree of twisting.

4.2 Opening angle

We noted earlier that the angular distribution of the collective photons depends on the photon helicity h=±1: Positive helicities tend to be associated with emission in the "northern" hemisphere, i.e. in the same direction as the spin of the mother nucleus, whereas photons with negative helicity are preferentially emitted into the "southern" hemisphere. This feature is intuitively expected: the photon tends to spin in the same sense as the emitting nucleus.

Consequently, the measurement of the helicities could provide information about the fragment spin direction. In particular, photon-photon correlation measurements could reveal information about the *relative* orientation of the spins of the two fragment partners.

As a quantitative illustration of this novel type of observable, we consider the distribution of the relative opening angle between two collective ($E2$) photons whose relative helicity is also being measured. (The term "relative" helicity refers to whether the two helicities are the same, $h_1h_2 = +1$, or opposite, $h_1h_2 = -1$.)

We concentrate on events leading to two even-even product nuclei for which (at least some of) the collective transitions can be experimentally identified and we then consider one such photon from each of the product partners. (The counting statistics can be improved significantly by utilizing that all such photon pairs contribute additively to the observable.)

The opening angle ψ_{12} between photon 1 and photon 2 is obtained from the relation $\cos\psi_{12} = \cos\theta_1\cos\theta_2 + \sin\theta_1\sin\theta_2\cos\phi_{12}$, where (θ_i, ϕ_i) is the direction of photon i and the difference between their azimuthal angles is $\phi_{12} = \phi_1 - \phi_2$. It is elementary to show [4] that if the angular distributions of the individual photons relative to a common axis are given by

$$\frac{dN_i}{d\cos\theta_i} = \sum_{n\geq 0} \alpha_n^{(i)} P_n(\cos\theta_i) \qquad (12)$$

then the distribution of the opening angle ψ_{12} is given by

$$P(\psi_{12}) = 2\sum_{n\geq 0} \frac{\alpha_n^{(1)}\alpha_n^{(2)}}{2n+1} P_n(\cos\psi_{12})\,. \qquad (13)$$

If only the positive perpendicular modes (wriggling) were populated at scission, the two fragment spins would be perfectly parallel. Conversely, if only the negative perpendicular modes (bending) were populated at scission, the two fragment spins would be exactly opposite. If any subsequent realignment of the spins could be ignored, the corresponding individual angular distributions (*w.r.t.* the angle between the photon and the spin direction of the light product nucleus) would then be of the form (12) with the respective coefficients being

$$\alpha_0^{(i)} = \tfrac{1}{2},\ \alpha_1^{(i)} = \pm\tfrac{1}{2}h_i,\ \alpha_2^{(i)} = -\tfrac{5}{14},\ \alpha_3^{(i)} = \mp\tfrac{1}{2}h_i,\ \alpha_4^{(i)} = -\tfrac{1}{7}, \qquad (14)$$

where upper signs refer to wriggling and lower signs refer to bending. With $\mu_{12} \equiv \cos\psi_{12}$, the distribution of the opening angle ψ_{12} between two $E2$ photons emitted from a pair of even-even product nuclei would therefore be

$$P^{\pm}(\psi_{12}) = \tfrac{1}{2}P_0(\mu_{12}) \pm \tfrac{1}{6}h_1h_2P_1(\mu_{12}) \qquad (15)$$
$$+\tfrac{5}{98}P_2(\mu_{12}) \pm \tfrac{1}{14}h_1h_2P_3(\mu_{12}) + \tfrac{2}{441}P_4(\mu_{12}).$$

Thus the odd-order terms change signs when the fragment spins change from being parallel to being anti-parallel. Because the signs of these terms also depend on the helicities through their product h_1h_2, those must be measured for the effect to be visible. (If the helicities were not detected, then the odd terms in $P(\psi)$ would average out.)

In order to examine the sensitivity of $P(\psi_{12})$ to the degree of agitation of the various dinuclear rotational modes, we have simulated a number of scenarios with FREYA. The results are illustrated in Fig. 5 below:

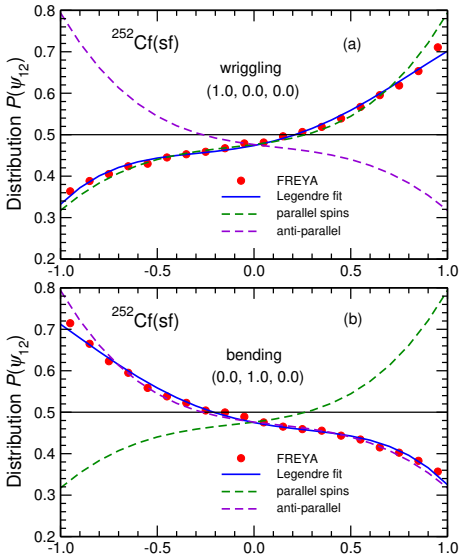

Figure 5. The distribution of the opening angle ψ_{12} between pairs of $E2$ photons emitted from even-even product partners, for two opposite scenarios for the dinuclear rotational modes at scission: Only wriggling is present (a) or only bending is present (b), for pairs with the same helicity. (The results for pairs with opposite helicities are reflected around $\psi_{12} = 90°$.) Each panel shows the result of the FREYA simulations (dots) and the associated Legendre fit (solid curve), as well as the result of perfectly parallel or anti-parallel fragment spins at the time of emission (dashed curves). (From Ref. [4].)

In each panel, the dashed curves show the form of $P(\psi_{12})$ if the two emitting fragments had their spins either perfectly aligned or perfectly anti-aligned at the time of the emisison of the detected photon, as given in Eq. (15).

In panel (a) only wriggling is included so the two fragments are formed with perfectly parallel spins and each of them are subsequently subjected to (relatively small) changes due to recoils from possible neutron evaporation and from any photon emissions prior to the emission of the detected photon. It is seen that the resulting opening-angle distribution is very close to the ideal form $P^{+}(\psi_{12})$, the most notable difference occurring at small opening angles, $\psi_{12} \approx 0°$.

Panel (b) shows the opposite extreme in which only bending is included, so the two fragments are formed with perfectly opposite spins. The resulting opening-angle distribution is then very close to the ideal form $P^{-}(\psi_{12})$, the most notable difference occurring at large opening angles, $\psi_{12} \approx 180°$.

The standard FREYA treatment includes wriggling and bending equally while excluding twisting. As discussed recently [13], this idealized scenario leads to fragment spins that are very nearly uncorrelated and the resulting distribution of their opening angle ψ_{12} is then nearly constant. This result is illustrated in Fig. 6 below.

That standard FREYA scenario is only a rough approximation to what would be theoretically expected, as discussed in Sect. 3. A more realistic scenario would likely have somewhat less bending and somewhat more twisting. However, because the reduction of bending is largely compensated by the admission of twisting, this change in the relative presence of the various rotational modes has an almost negligible effect on $P(\psi_{12})$.

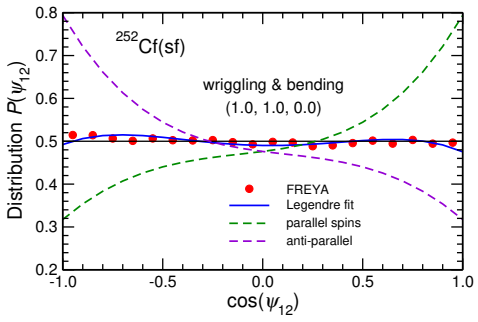

Figure 6. In a display similar to those in Fig. 5 is shown the distribution of the opening angle ψ_{12} between pairs of $E2$ photons emitted from even-even product partners, for the standard FREYA scenario where wriggling and bending are fully populated while there is no twisting. Also shown are the results for perfectly parallel or anti-parallel fragment spins at the time of the photon emission (dashed curves). (From. Ref. [4].)

The above results suggest that measurements of photons with identified helicities could provide a powerful means for probing the relative direction of the angular momenta of fission fragment partners.

5 Concluding remarks

The normal modes of rotation in the dinuclear complex at scission provide a convenient framework for discussing the fission fragment angular momenta. Their relaxation times, as given by the nucleon exchange transport model, suggest that wriggling should be equilibrated at scission. Bending may not be fully equilibrated but its role increases with the mass asymmetry and may also be larger for events with small fragment kinetic energies. Twisting plays only a minor role that may increase with energy; its presence may be probed in a modern Wilhelmy-type experiment [1].

Acknowledgments

We acknowledge helpful communications with B. Back, S. Marin, K.H. Schmidt, C. Schmitt, and J.B. Wilhelmy. This work was supported by the Office of Nuclear Physics in the U.S. Department of Energy's Office of Science under Contracts No. DE-AC52-07NA27344 (RV) and DE-AC02-05CH11231 (JR).

References

[1] J. B. Wilhelmy, E. Cheifetz, R. C. Jared, S. G. Thompson, H. R. Bowman, J. O. Rasmussen, Phys. Rev. C **5**, 2041 (1972).
[2] J. Wilson *et al.*, Nature (London) **590**, 566 (2021).
[3] T. Døssing, S. Åberg, M. Albertsson, B. G. Carlsson, J. Randrup, Phys. Rev. C **109**, 034615 (2024).
[4] J. Randrup, T Døssing, R. Vogt, Phys. Rev. C 1069, 014609 (2022).
[5] J. R. Nix, W. J. Swiatecki, Nucl. Phys. **71**, 1 (1963).
[6] T. Døssing, J. Randrup, Nucl. Phys. A **433**, 215 (1985).
[7] J. Randrup, Nucl. Phys. A **383**, 468 (1983).
[8] J. Błocki, Y. Boneh, J. R. Nix, J. Randrup, M. Robel, A. J. Sierk, W. J. Swiatecki, Ann. Phys. **113**, 330 (1978).
[9] J. Randrup, R. Vogt, Phys. Rev. C **89**, 044601 (2014).
[10] J. M. Verbeke, J. Randrup, R. Vogt, Comp. Phys. Comm. **191**, 178 (2015).
[11] J. M. Verbeke, J. Randrup, R. Vogt, Comp. Phys. Comm. **222**, 263 (2018).
[12] A. Wolf, E. Cheifetz, Phys. Rev. C **13**, 1952 (1976).
[13] J. Randrup, R. Vogt, Phys. Rev. Lett. **127**, 062502 (2021).